


Proceeding Paper

Bioengineered Monoclonal Antibody Chitosan–Iron Oxide Bio-Composite for Electrochemical Sensing of *Mycobacterium tuberculosis* Lipoprotein [†]

Resmond L. Reaño ^{1,*} , Glenson R. Panghulan ¹, Clydee Ann T. Hernandez ¹ and Jeffrey P. Tamayo ²

¹ Department of Engineering Science, College of Engineering and Agro-Industrial Technology, University of the Philippines Los Baños, Los Baños 4031, Philippines

² Central Analytical Services Laboratory, National Institute of Molecular Biology and Biotechnology, University of the Philippines Los Baños, Los Baños 4031, Philippines; jptamayo1@up.edu.ph

* Correspondence: rleano@up.edu.ph

[†] Presented at the 10th International Electronic Conference on Sensors and Applications (ECSA-10), 15–30 November 2023; Available online: <https://ecsa-10.sciforum.net/>.

Abstract: In this study, an electrochemical immunosensor for the detection of the 19 kDa *Mycobacterium tuberculosis* lipoprotein LpqH was developed using a monoclonal antibody immobilized on a chitosan-coated iron oxide bio-composite. The bio-composite is composed of magnetic iron oxide at its core and a non-magnetic thin film on the surface formed by chitosan, providing the chemistry for monoclonal antibody immobilization. Cyclic voltammetry was used to characterize and test the immunosensor assembly. Electrochemical measurements showed a strong relationship between the LpqH concentration in phosphate-buffered saline solution and the measured anodic peak current. The electrochemical immunosensor showed a limit of detection equal to 40 µg/mL (2 µM) LpqH.

Keywords: immunosensor; chitosan-coated iron oxide; monoclonal anti-LpqH; bio-nanocomposite; point-of-care testing; tuberculosis



Citation: Reaño, R.L.; Panghulan, G.R.; Hernandez, C.A.T.; Tamayo, J.P. Bioengineered Monoclonal Antibody Chitosan–Iron Oxide Bio-Composite for Electrochemical Sensing of *Mycobacterium tuberculosis* Lipoprotein. *Eng. Proc.* **2023**, *58*, 23. <https://doi.org/10.3390/ecsa-10-16065>

Academic Editor: Francisco Falcone

Published: 15 November 2023



Copyright: © 2023 by the authors. Licensee MDPI, Basel, Switzerland. This article is an open access article distributed under the terms and conditions of the Creative Commons Attribution (CC BY) license (<https://creativecommons.org/licenses/by/4.0/>).

1. Introduction

Mycobacterium tuberculosis (*MTb*) is the cause of tuberculosis (TB), an airborne infectious disease that infects humans as a primary host [1]. *MTb* is an ancient pathogen that has been persistent due to its complex survival strategies in the living host and the environment. It has developed a repertoire of culture filtrate antigens (Ags) that multiply as the disease progresses [2,3]. Among the notable TB antigens and biomarkers are CFP10, ESAT6, LAM, HBHA, HspX, and LpqH, which can be detected using a serologic immunoassay [1].

LpqH is a mycobacterial lipoprotein, a bacterial secretion that is composed of membrane-anchored proteins characterized by a lipobox motif [4]. LpqH, also known as the 19-kDa antigen, is an *MTb* outer membrane-anchored glycol-lipoprotein that has been shown to exhibit immunosuppressive functions. It has been well established that LpqH interacts with TLR1/TLR2 on the macrophage cell surface, thereby regulating the host immune response. Aside from that, LpqH acts as an adhesin that establishes the colonization and infection of *MTb* onto the host cell surface [5].

Antibodies (Abs) have become a popular candidate for biosensor development due to their high affinity and specificity to their targets. Enzyme-linked immuno-sorbent assay (ELISA), the gold standard for all immunoassays, is still popular and used worldwide in different fields of application, particularly in clinical diagnostics. With the advancement in analytical and bioanalytical chemistry, the incorporation of antibodies directly to the signal transducer's surface gave birth to a combined immunoassay and biosensor technology termed an immunosensor [6,7]. An immunosensor is a biosensor that uses an antibody as a capture element, wherein such antibody forms a stable immunocomplex with the

antigen, which results in the generation of a measurable signal given by the transducer. In contrast, in an immunoassay, the signal recognition from Ag-Ab interaction takes place elsewhere [8].

This study aimed to develop an electrochemical immunosensor for *MTb* LpqH detection using a bio-composite composed of a monoclonal antibody that is specific to LpqH (anti-LpqH) incorporated on iron oxide nanoparticles via bioengineering techniques. The study also aimed to assess the affinity of the anti-LpqH and the limit of detection of the proposed electrochemical setup. To our knowledge, there is no study available on electrochemical immunosensors for *MTb* LpqH detection with or without clinical trials. The procedure also provides a cheap alternative to handling biological molecules by using magnetic iron oxide nanoparticles and chitosan as crosslinkers. The future direction of the study includes developing a more sensitive protocol for *MTb* LpqH detection by improving the electrode assembly and using electroactive labels.

2. Materials and Methods

The *Mycobacterium tuberculosis* 19 kDa recombinant and conserved form lipoprotein, an antigen precursor (LpqH), and the monoclonal anti-LpqH, IT-54, produced in vitro were obtained through BEI Resources, NIAID, NIH. The lipoprotein and the anti-LpqH were diluted using PBS Buffer (10 mM phosphate, 138 mM NaCl, and 2.7 mM KCl at pH 7.4) purchased from Sigma-Aldrich (Burlington, MA, USA) in powdered form. The tween 20 used in creating an emulsion and for making 0.05% *v/v* PBS-tween buffer at pH 7.4 for blocking was purchased from Promega (Madison, WI, USA). All other chemicals, including acids and bases used, were ACS grade and purchased from Sigma-Aldrich, particularly those used for iron oxide and chitosan synthesis.

2.1. Synthesis and Characterization of Monoclonal Antibody Immobilized on Chitosan-Coated Iron Oxide (AbMNP)

Iron oxide (chemical formula: Fe_3O_4 , abbr. as IONP) particles were prepared using FeCl_3 and FeSO_4 and following the methodology described by Hierro et al., 2018 [9]. Chitosan was prepared using shrimp shells obtained from the local market and sun-dried for 2–3 days. The shells were demineralized, and chitin was extracted via the process described by Varun et al., 2017 [10].

A 200 g of as-prepared IONP was mixed with 55 mL mineral oil, 1.2 mL tween 20, and 10 mL 1% *w/v* CS, creating an emulsion. The mixture was sonicated and stirred for 35 min. After recovering the CS-IONP bio-composite and washing with double distilled water, 3 mL of 25% glutaraldehyde solution was added, and the mixture was stirred for 5 hrs. Anti-LpqH (100 $\mu\text{g}/\text{mL}$) was added to the optimum amount of glutaraldehyde-activated CS-IONP, and the solution was incubated overnight at 4 °C. The AbMNP was isolated, PBS-tween was added for blocking, and PBS solution for storage.

The microstructure of the two samples, the bare IONP and the AbMNP, were observed using a Field Emission Scanning Electron Microscope (JSM-IT500HR, JEOL, Tokyo, Japan). The voltage used was 3.0 kV, with each sample observed at 1000 \times and 15,000 \times magnification.

The samples were also tested using a Fourier transform infrared spectrophotometer or FTIR (Shimadzu IR Prestige-21, Kyoto, Japan) with attenuated total reflectance accessory.

2.2. Enzyme-Linked Immunosorbent Assay (ELISA) and Calculation of Dissociation Constant

ELISA was performed using the conventional process, with IgG-Alkaline Phosphatase and pNPP tablet (Sigma, Burlington, MA, USA). The LpqH antigen (50 μL at 20 $\mu\text{g}/\text{mL}$) was immobilized on a Corning[®] Polystyrene High Bind Microplate (Corning Inc., New York, NY, USA) by incubation overnight at 4 °C. PBS-tween (200 μL at 0.05% *v/v*) solution was added to the well and incubated for 1 h at room temperature to prevent non-specific binding. After blocking, the wells were washed with PBS-tween. Then, 50 μL of anti-LpqH in binding buffer solution at various dilutions were added to each separate well with immobilized LpqH. The microplate was incubated for 1 h at 37 °C with gentle shaking.

Each well was washed thrice with the PBS buffer. Then, the standard ELISA protocol for the addition of IgG-AP and pNPP was followed until a deep yellow color was developed. The absorbance was measured at 405 nm. The apparent dissociation constant or K_d^{app} was calculated following the method described by Orosz and Ovádi (2002) [11].

2.3. Cyclic Voltammetry and the Limit of Detection

A single-use screen-printed carbon electrode (SPCE) (Biogenes Technologies, Kuala Lumpur, Malaysia) was used to perform the electrochemical measurements. Various concentrations of LpqH were prepared and allowed to interact with the monoclonal anti-LpqH on AbMNP. Cyclic voltammetry (CV) was performed using an electrochemical workstation Em4Stat (PalmSens, Utrecht, The Netherlands). The applied potential varied between -1 and 1 V with a scan rate of 50 mV/s. All electrochemical measurements were performed using $1 \times$ PBS buffer. The limit of detection was calculated using the linearized curve of the anodic peak current.

All calculations (linear regression, dissociation constant, limit of detection, and statistical analyses) were performed using a Python script.

3. Results

3.1. Synthesis and Characterization of Monoclonal Antibody Immobilized on Chitosan-Coated Iron Oxide (AbMNP)

Figure 1 shows the FTIR transmittance spectra of the as-prepared IONP and the AbMNP. The transmittance spectra within the 4000 – 400 cm^{-1} range were recorded for the samples. The wide band gap from 3700 to 3000 cm^{-1} and peak at 1645 cm^{-1} is attributed to the stretching vibration of $-\text{OH}$ groups on the surface of the particles. The peak at 2937 cm^{-1} corresponds to the $-\text{CH}$ bond of CH_2 bending. The peaks at 1455 cm^{-1} and 1366 cm^{-1} represent the symmetric $-\text{CH}_3$ deformation of chitosan. The peaks at 569 cm^{-1} and 459 cm^{-1} are typical of $\text{Fe}-\text{O}$ that correspond to the vibrations of tetrahedral $\text{Fe}-\text{O}$ and octahedral $\text{Fe}-\text{O}$ bonds. The band at 1070 cm^{-1} is attributed to the $\text{C}-\text{OH}$ and $\text{C}-\text{O}-\text{C}$ vibrations of the chitosan ring.

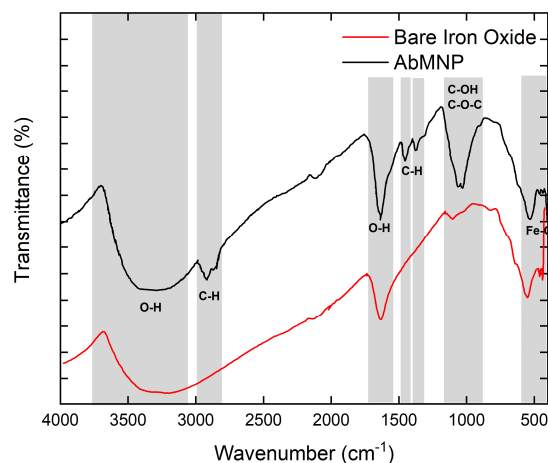


Figure 1. FTIR spectra of bare Iron oxide (Fe_3O_4) and the monoclonal anti-LpqH covalently bonded on magnetic iron oxide via chitosan–glutaraldehyde crosslinking (AbMNP).

The structural morphology of the IONP was investigated by scanning electron microscopy (SEM). Figure 2 depicts the surface images of the particles. Figure 2a,b shows the as-prepared IONP consisting of agglomerated nanoparticles. Figure 2c,d showed that the nanoparticles are coated with chitosan molecules, as shown with smoother lumps.

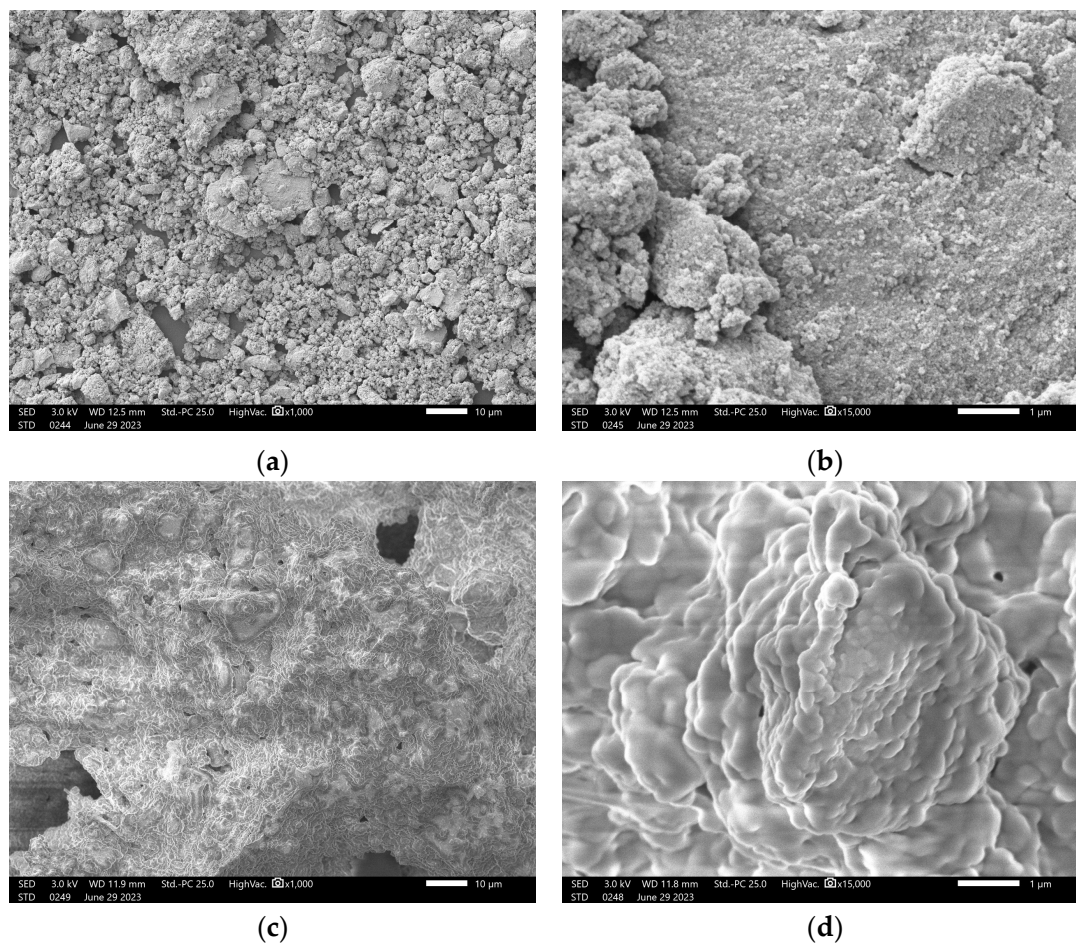


Figure 2. The SEM images of bare IONP at (a) 1000 \times and (b) 15,000 \times magnification, and AbMNP at (c) 1000 \times and (d) 15,000 \times magnification.

3.2. Determination of the Apparent Dissociation Constant (K_d) of the Monoclonal Anti-LpqH Using ELISA

ELISA was performed to provide a quantitative analysis of the interaction of the anti-LpqH and the *MTb*. lipoprotein LpqH by calculating the apparent dissociation constant (K_d^{app}) of the immunocomplex formation. Figure 3a shows the relative absorbance measured for each anti-LpqH dilution titrated with the lipoprotein. The IC_{50} was obtained at 50% relative absorbance ($i = 0.50$) and is equal to 3.140, with the anti-LpqH exact dilution of 7.24×10^{-4} . The IC_{50} was used to calculate the corrected parameters of the linearized curve, with the slope $m = \left(\frac{1}{K_d^{app}} \right) = 100.00$ and the y-intercept (b) = -1.8550 . The value of $\frac{1}{K_d^{app}}$ implies that with 1000-fold dilution, an effective performance of the anti-LpqH can be anticipated in detecting the LpqH lipoprotein using ELISA. This value was used as the basis for the dilution of the anti-LpqH used in the electrochemical biosensor.

3.3. Cyclic Voltammetry and Determination of Limit of Detection

The resulting voltammogram from testing various *MTb* LpqH concentrations is shown in Figure 4a. The shift in the measured anodic current is highly recognizable as the concentration of the antigen increases. Using the anodic peak current, a linear curve was created as shown in Figure 4b. The limit of detection was computed as 2.0923 μM (39.7545 $\mu\text{g/mL}$) *Mtb* LpqH.

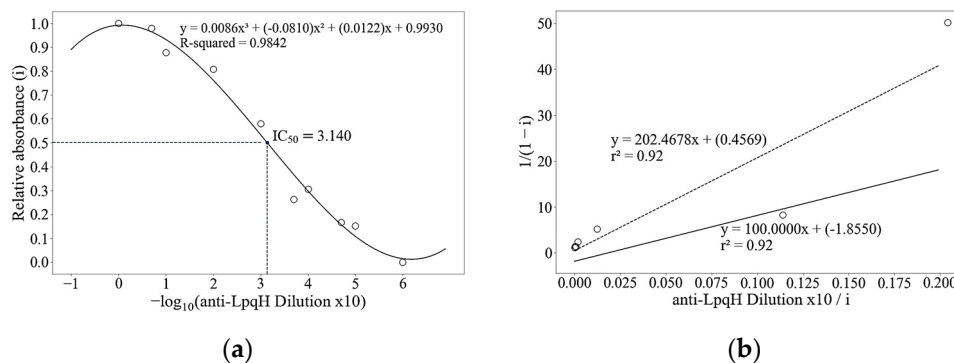


Figure 3. (a) Plot of relative absorbance, i vs. $-\log_{10}(10 \cdot \text{dilution})$, data obtained through ELISA. (b) The parameters of the linearized curve are shown following the method [11]. The corrected slope is $\left(\frac{1}{K_d^{app}}\right) = 100.00$, upon using IC_{50} compute for the corrected y-intercept (-1.8550) , which was used as linear regression constraint (Pearson correlation = 0.92).

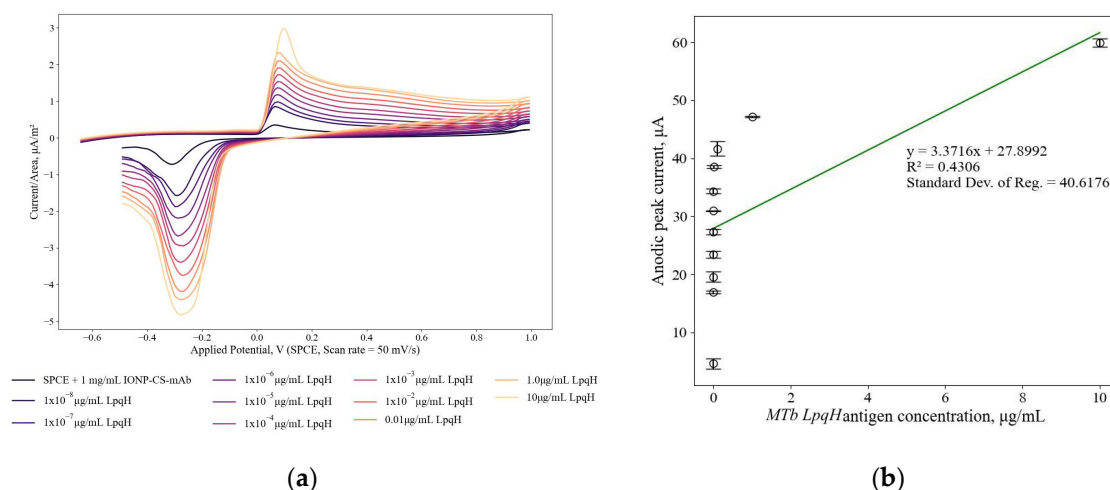


Figure 4. (a) Voltammograms of TB lipoprotein LpqH antigen precursor detection using AbMNP as bioreceptor, measured using 50 mV/s scan rate and screen-printed carbon electrode. (b) The plot of the anodic peak current with error bars and linearized curve for estimating the limit of detection.

4. Discussion

The AbMNP bio-composite acts as a nanocarrier and captures the target *MTb* LpqH. Using IONP as its magnetic core, AbMNP is easy to collect, wash, and handle using a simple magnet. Reports showed that IONP is electrocatalytic; thus, it can promote the breakdown or release of the anti-LpqH upon interacting with the antigen and/or while current is applied. Biological molecules are non-conductive and their release from the bio-composite’s surface supports electric conduction. The LOD can be improved further by optimizing the density of the anti-LpqH or by incorporating an electroactive or electrocatalytic label that can induce a redox reaction with the Ag-Ab interaction.

Author Contributions: Conceptualization, R.L.R. and C.A.T.H.; methodology, R.L.R., G.R.P. and J.P.T.; formal analysis, R.L.R., G.R.P. and C.A.T.H.; investigation, R.L.R. and C.A.T.H.; resources, R.L.R. and J.P.T.; writing—original draft preparation, R.L.R., G.R.P. and C.A.T.H.; writing—review and editing, R.L.R.; supervision, R.L.R. and J.P.T.; project administration, R.L.R., G.R.P., C.A.T.H. and J.P.T.; funding acquisition, R.L.R. and J.P.T. All authors have read and agreed to the published version of the manuscript.

Funding: This research was funded by the Department of Science and Technology (DOST)—Philippine Council for Health Research and Development. Project Title: Development of aptamer based colorimetric and electrochemical point of care type diagnostic test for pulmonary TB and latent TB infection.

Institutional Review Board Statement: Not applicable.

Informed Consent Statement: Not applicable.

Data Availability Statement: Data are contained within the article.

Acknowledgments: The authors would like to acknowledge the BEI Resources, NIAID, NIH, USA for antigens and antibodies used in this study and the NITL, BIOTECH, UPLB, PH for technical support.

Conflicts of Interest: The authors declare no conflict of interest.

References

1. Krishnananthasivam, S.; Li, H.; Bouzeyen, R.; Shunmuganathan, B.; Purushotorman, K.; Liao, X.; Du, F.; Friis, C.G.K.; Crawshay-Williams, F.; Boon, L.H.; et al. An Anti-LpqH Human Monoclonal Antibody from an Asymptomatic Individual Mediates Protection against Mycobacterium Tuberculosis. *NPJ Vaccines* **2023**, *8*, 127. [[CrossRef](#)] [[PubMed](#)]
2. Samanich, K.M.; Keen, M.A.; Vissa, V.D.; Harder, J.D.; Spencer, J.S.; Belisle, J.T.; Zolla-Pazner, S.; Laal, S. Serodiagnostic Potential of Culture Filtrate Antigens of Mycobacterium Tuberculosis. *Clin. Diagn. Lab. Immunol.* **2000**, *7*, 662–668. [[CrossRef](#)] [[PubMed](#)]
3. Tucci, P.; Portela, M.; Chetto, C.R.; González-Sapienza, G.; Marín, M. Integrative Proteomic and Glycoproteomic Profiling of Mycobacterium Tuberculosis Culture Filtrate. *PLoS ONE* **2020**, *15*, e0221837. [[CrossRef](#)] [[PubMed](#)]
4. Becker, K.; Sander, P. *Mycobacterium tuberculosis* Lipoproteins in Virulence and Immunity—Fighting with a Double-Edged Sword. *FEBS Lett.* **2016**, *590*, 3800–3819. [[CrossRef](#)] [[PubMed](#)]
5. Chatterjee, S.; Kundapura, S.V.; Basak, A.J.; Mukherjee, D.; Dash, S.; Ganguli, N.; Das, A.K.; Mukherjee, G.; Samanta, D.; Ramagopal, U.A. High-Resolution Crystal Structure of LpqH, an Immunomodulatory Surface Lipoprotein of Mycobacterium Tuberculosis Reveals a Distinct Fold and a Conserved Cleft on Its Surface. *Int. J. Biol. Macromol.* **2022**, *210*, 494–503. [[CrossRef](#)] [[PubMed](#)]
6. Popov, A.; Brasiunas, B.; Kausaite-Minkstimiene, A.; Ramanaviciene, A. Metal Nanoparticle and Quantum Dot Tags for Signal Amplification in Electrochemical Immunosensors for Biomarker Detection. *Chemosensors* **2021**, *9*, 85. [[CrossRef](#)]
7. Jafari, M.; Hasanzadeh, M.; Solhi, E.; Hassanpour, S.; Shadjou, N.; Mokhtarzadeh, A.; Jouyban, A.; Mahboob, S. Ultrasensitive Bioassay of Epitope of Mucin-16 Protein (CA 125) in Human Plasma Samples Using a Novel Immunoassay Based on Silver Conductive Nano-Ink: A New Platform in Early Stage Diagnosis of Ovarian Cancer and Efficient Management. *Int. J. Biol. Macromol.* **2019**, *126*, 1255–1265. [[CrossRef](#)] [[PubMed](#)]
8. Mollarasouli, F.; Kurbanoglu, S.; Ozkan, S.A. The Role of Electrochemical Immunosensors in Clinical Analysis. *Biosensors* **2019**, *9*, 86. [[CrossRef](#)] [[PubMed](#)]
9. del Hierro, I.; Pérez, Y.; Fajardo, M. Silanization of Iron Oxide Magnetic Nanoparticles with Ionic Liquids Based on Amino Acids and Its Application as Heterogeneous Catalysts for Knoevenagel Condensation Reactions. *Mol. Catal.* **2018**, *450*, 112–120. [[CrossRef](#)]
10. Varun, T.K.; Senani, S.; Jayapal, N.; Chikkerur, J.; Roy, S.; Tekulapally, V.B.; Gautam, M.; Kumar, N. Extraction of Chitosan and Its Oligomers from Shrimp Shell Waste, Their Characterization and Antimicrobial Effect. *Vet. World* **2017**, *10*, 170–175. [[CrossRef](#)] [[PubMed](#)]
11. Orosz, F.; Ovádi, J. A Simple Method for the Determination of Dissociation Constants by Displacement ELISA. *J. Immunol. Methods* **2002**, *270*, 155–162. [[CrossRef](#)] [[PubMed](#)]

Disclaimer/Publisher’s Note: The statements, opinions and data contained in all publications are solely those of the individual author(s) and contributor(s) and not of MDPI and/or the editor(s). MDPI and/or the editor(s) disclaim responsibility for any injury to people or property resulting from any ideas, methods, instructions or products referred to in the content.